A Multiscale-Multiphysics Model for Axon Pathfinding Simulation, the Example of the Olfactory System

Giacomo Aletti[1], Paola Causin[1], and Giovanni Naldi[*,1]
[1]Dipartimento di Matematica "F. Enriques", Università degli studi di Milano
*Corresponding author: via Saldini 50, 20133 Milano, giovanni.naldi@unimi.it

Abstract: In the developing embryo, neurons form connections by projecting axons to appropriate target areas. The projection process includes neurite elongation, resulting from the assembly of new cytoskeletal material at the free end of the axon , a complex cascade of steering decisions, driven by signals in the surrounding environment, and the biomechanical properties of the extracellular matrix. In this work we focus on the early development of the olfactory nerve. In particular, we discuss a mathematical and numerical multiscale framework aimed at obtaining a description of the morphological organization of the axons at the first steps of the olfactory system formation. Here we also discuss possible applications and generalizations with the numerical difficulties in the computational approach.

Keywords: Axon guidance, Growth cone navigation, Filopodia model, extracellular matrix, Multiscale model.

1. Introduction

In the developing nervous system, axons find the targets they will innervate navigating through the extracellular environment. Pathfinding crucially relies on chemical cues and, among the others, guidance by gradients of diffusible ligands plays a key role see, e.g. [1,2,3]). The structure of the axon deputed to detect and transduce extracellular cues is the growth cone, located at the axon tip. The growth cone is provided of several filopodia, small filaments that protrude in a fan-shaped array from the lamellar veils surrounding the central nucleus. Filopodia are highly active structures that provide multiple functions [4,5]. On the one side, they probe the environment acting as sensor: due to their high area to volume ratio, individual filopodia can read extracellular chemical cues with a high sensitivity. Moreover, they have been recognized to play an essential role in detecting contact-mediated signals as well as graded chemotropic signals. On the other side, filopodia can adhere to the substratum by their tips and exert a pull force on the growth cone.

Here we briefly present a mathematical and numerical framework aimed at obtaining a description of the macroscopic growth cone trajectories in a possibly complex environment. In the present model, the continuous movement of the axon growth cone observed at a coarse time scale is obtained on the base of a lumped description of the filopodia dynamics. Namely, we describe the joint action of the filopodia as a lumped 1D mass-spring system, that pulls the growth cone and the trailing axon body in the direction of the perceived cues. The parameters entering the lumped model are fitted on the base of the axonal response in certain well studied conditions. In particular, as a model of response we consider here the turning angles obtained from experiments in which the axons are exposed to a graded attractive concentration of ligand [6,7]. The mechanical effects of the matrix are also investigated, extending the model to the case where the surrounding matrix is undergoing a deformation field. We point out that significant differences in the resulting morphology are shown with respect to the fixed geometry case. In order to tackle the problem in a variegated scenario, more similar to the in vivo conditions, more sophisticated numerical techniques are required. Approximate solutions of partial differential equation systems in the resulting mathematical model with finite element techniques are introduced to carry out numerical simulations that describe the phenomenon. This complex multiscale problem looks like a good opportunity for potential COMSOL Multiphysics.

2. From cues to axon movements

2.1 Lumped model of filopodia dynamics

In the developing nervous system, axons find the targets they will innervate navigating through the extracellular environment. Pathfinding crucially relies on chemical cues and, among the others,

guidance by gradients of diffusible ligands plays a key role. Detection and transduction of navigational cues is mediated by the growth cone (GC), a highly dynamic structure located at the axon tip. The cascade that leads to motility decisions is initiated by binding of the ligand with receptors located on the GC surface and on filopodia, thin filaments that protrude out from the distal part of the GC. In the olfactory system, individual axons of olfactory receptor neurons (ORNs) located in the epithelium lining the nasal cavity project to the olfactory bulb where they synapse on the dendrites of second-order neurons within globular structures of neuropil - glomeruli It was recently discovered that all of the axons from ORNs expressing the same odorant receptor gene converge onto two (or a few) glomeruli in the bulb. The location of these glomeruli is bilaterally symmetrical and invariant across animals. However, little is understood about the mechanisms in the olfactory bulb governing such precise topographical targeting by ORN axons. Continual neurogenesis in the subventricular zone of postnatal and adult forebrain has been well documented, but the mechanisms underlying cell migration differentiation from this region are poorly understood [8]. In Figure 1. we briefly described the main factors involves in migration, guidance and organization of axon projection. We represent each axon as a 1D elastic body immersed in the extracellular matrix, modeled in turn as a 2D continuum deformable body. The axon is supposed to be clamped at a boundary of the matrix and to grow away from this position with an intrinsic growth rate.

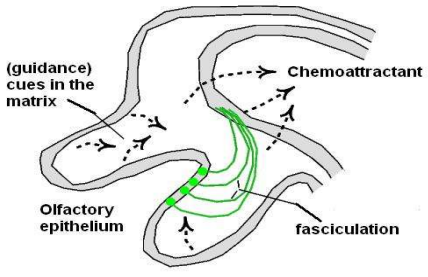

Figure 1. The whole process of the early formation of the olfactory nerve.

Unless otherwise influenced, axons show a general tendency to extend in straight lines, by virtue of the inherent rigidity of their internal microtubular structure. In presence of chemical ligand, binding with receptors distributed on filopodia and growth cone outer surface occurs. This fact triggers a sequence of complex intracellular signaling mechanisms, a macroscopic result of which is the redistribution of filopodia in a biased way around an angular sector induced by the signal. We represent the joint pull action of filopodia as a lumped 1D mass-spring system. The spring, with its internal stiffness, is connected to the filopodia mechanical properties, while the mass represents the inertial effect of the trailing growth cone, pulled away from its original trajectory.

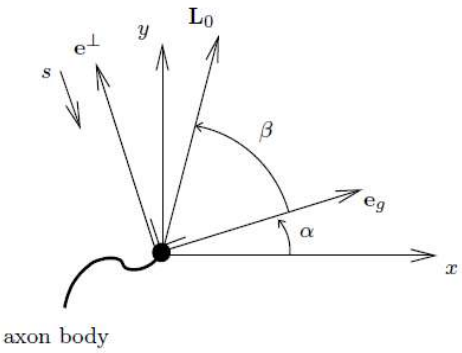

Figure 2. Notation for the lumped model of filopodia and growth cone.

With reference to Figure 2, Let $\mathbf{L}_0$ the vector representing he initial length of the spring (direction and modulus), and let $\mathbf{v_g} = v_g\, \mathbf{e_g}$ be the growth cone velocity. We consider the modulus v_g to be a given constant quantity. The unit vector $\mathbf{e_g}$ forms an angle α with respect to the horizontal direction. The unit vector $\mathbf{e_r}$ forms an angle β with $\mathbf{e_g}$. We model the perturbation to the motion induced by extracellular cues acting only along the direction $e\perp$, with abscissa s, orthogonal to $\mathbf{e_g}$. This means to consider the effect of the spring projected along this direction. Let $\omega=\sqrt{(k/m)}$ the harmonic pulsation, k and m being the spring stiffness and the body mass, respectively. Moreover, let δt be the time scale of the growth cone turning, under the hypothesis $\omega\, \delta t \ll 1$, the following differential system of equations describe the trajectory evolution of the growth cone position $\mathbf{X_d} = \mathbf{X_d}(t)$, as a continuous phenomenon for $0 \le t \le T$,

$$\dot{X}_d = v_g,\ dv_g = (e_g \wedge L_0) \wedge e_g \left(\frac{\omega^2}{2}\right) dt$$
$$X_d(0) = x_d^0,\ v_g(0) = v g e_g^0 \qquad (1)$$

where x_d^0 and v_g^0 are the initial position and direction of the axon growth cone, respectively.
We approximated the system (1) with a numerical integration scheme based on Runge-Kutta method. Moreover, in vitro experiments are carried, establishing an attractive diffusible ligand gradient in a substrate where axon explants are let grown. Axon trajectories are observed turning towards the increasing gradient and turning angles are measured. These measurements deal for the most part with the response to a single graded chemotropic substance.

2.2 ligand fields

The concentration field distribution of a diffusible substance can be modeled as the result of a diffusion-degradation process occurring after the substance has been released at rate q from target areas. We consider the following system

$$-D\Delta c(x)+kc(x)=\sum_{j=1}^{N} 1_{A_j} q, \quad (2)$$
$$\frac{\partial c}{\partial n}=0 \; on \; \partial\Omega_M,$$

where the first equation is for $x\in\Omega_M$ the bidimensional computational domain, D is the diffusion coefficient and k the degradation coefficient and where 1_{Aj} is the characteristic function such that for every subset A_j of Ω_M has value 1 at points of A_j and 0 at points of $\Omega_M \setminus A_j$. Standard no--flux conditions are imposed on the boundaries. Ligands are supposed not to mutually interact in the substrate. System (2) describes the stationary state of the diffusion process. To approximate system (2), we use the Finite Element Method (FEM), with linear interpolation functions (P_1 elements) on a triangular mesh as available in the basic COMSOL Multiphysics.
Axons response in presence of multiple cues, this is a complex situation, especially in view of the fact the response of a neuron can be mediated not only by the temporal graded expression of receptors for the single ligand, but also by the interplay of receptors. We do not address detailed intracellular pathways, but we aim rather at a description of the downstream effect on directional movement. Namely, we introduce weights $\lambda_i(t)$\$ that are related to the time availability of receptors for the corresponding cue. Accordingly, they model the time-dependent activity of receptors, possibly influenced by the competition with other receptors (for example in a receptor--mediated silencing mechanism). The equivalent spring mean length vector l_0 $\mathbf{e}_r$ results from the weight combination.

2.3 Deformation field induced by the extracellular matrix

Mechanical properties of axons and of their surrounding environment are issues gaining increasing importance. A microneedle locally applying a force induces deformations on axon shaft. Behavior under tension and recover from deformations allow to characterize the main axon mechanical properties [9] Transduction pathways are being studied that explain how the cytoskeleton reorganizes following to an applied tension.
the initial time is denoted by Ω_M^0 and it will be referred to as the reference configuration. The deformed domain at the time t is denoted by $\Omega_M(t)$. By introducing a Cartesian reference frame at a fixed origin O, the components of position vectors in each configuration being measured along these axes. The smooth deformation function φ maps any point $\mathbf{X}$ in Ω_M^0 onto the corresponding point $\mathbf{x}=\varphi(\mathbf{X},t)$. The map φ is assumed to possess continuous derivative with respect to position and time and to be invertible. The field $\mathbf{U}(\mathbf{X},t)=\mathbf{x}(\mathbf{X},t)-\mathbf{X}$ represents the displacement field of a particle. The velocity of axons gaining their way through the deforming matrix, is the superposition of their intrinsic growth speed and of the matrix speed. We suppose axons to passively follow the deformations imposed by the matrix (a wide spectrum of different behaviors could be analyzed with this respect). On the reference domain, the series of position of the axon head (the axon trajectory) is represented by the material curve $\mathbf{\Gamma}$, and the the velocity being given by the total time derivative

$$\dot{X}_d(t)=v_g(t)+v_\varphi(t),$$

where it is now present the additional term $v_\varphi(t)$, representing the time rate variation of the matrix shape.
In reality, the displacement field of the developing tissue is itself an unknown of the problem, resulting from several complex processes of growth, remodeling and morphogenesis. In this work, we model the mesenchyme as a unique deformable elastic

body that undergoes large deformations, this hypothesis being general enough to allow for a series of successive improvements in more refined models. For reasons of simplicity we do not consider mass sources or sinks. The forcing term is represented by an imposed motion of the (computational) boundaries. When disposing of digitally segmented section from laboratory experiments, the imposed motion can be directly inferred from data segmentation. This will be the object of a future work. As usual in a large deformation regime, the mechanical problem
at each time step is mapped to the reference configuration $\Omega_M^{0.}$ The boundary of Ω_M^0 is partitioned in a part Γ_D, where Dirichlet boundary conditions are prescribed and a part Γ_N, where Neumann no-stress boundary conditions are prescribed. The deformation takes place in a manner slow enough to allow for neglecting inertial terms. Moreover, as common in biological applications, we suppose null body forces. The mathematical model on the reference configuration reads

$$\begin{aligned} -\nabla_X \cdot T &= 0 \; on \; \Omega_M^{0,} \\ U &= \hat{U} \; on \; \hat{\Gamma}_D, \\ T \cdot \hat{n_M} &= 0 \; on \; \hat{\Gamma}_N, \end{aligned} \qquad (3)$$

where $\tilde{\tilde{n}}_M$ denotes the outward normal on the boundary of the reference configuration, T is the first Piola-Kirchoff stress tensor and $\tilde{\tilde{U}}$ is a prescribed displacement field. We consider the extracellular matrix to be an hyperelastic material, so that the stress tensor is given by the derivative of an internal stored energy function.
The choice of the particular form of the internal stored energy does not change the setting of the problem. Here, we adopt the simplest isotropic elastic St.Venant--Kirchhoff model: the elastic strain energy is a function of body deformation only (and not of deformation history), and at any location the response of the material in a stress--strain experiment is the same in all directions.
To discretize system (3) in the complex geometry of the developing embryo, we use again the FEM. The elastic body is represented as a mesh consisting of triangles. A deformed configuration is specified by the displacements of the n mesh vertices and is approximated by piecewise linear functions.

4. Some numerical studies

We present the results of the complete model (1), (2), (3) while in the subsequent series of tests, we investigate the effect of turning off a single mechanism.
A result of the simulation using the complete model are shown in Figure 3, at initial, half and final time, respectively. We consider 500 axons, randomly seeded along the bottom boundary and assigned different birth times. A prescribed motion (amounting at the final time at about the 20% of the initial vertical dimension for each side) is imposed to the top and bottom borders.
A weak attractive diffusible cue is placed in the top-central part of the domain. Repulsive cues are placed close to the corners.

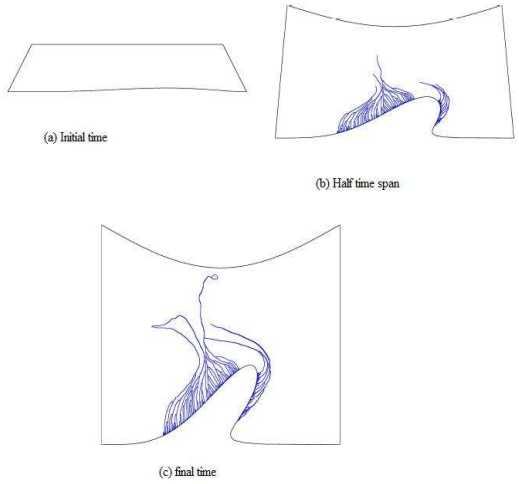

Figure 3. Axon morphology with the complete model, the geometry is evolving.

In Figure 4 we show the morphology of the nerve when fasciculation is turned off. Notice that in this simulation only 50 axons are considered. Diffusible chemical cues drive axons near but, in absence of homophilic attraction, they do not form a coherent structure and they depart in a fan.
When diffusive cues are turned off, axons tend to grow straight and to disperse in the extracellular matrix. Axon fasciculation is observable at a certain degree, being promoted by random movements and geometrical neighborhood. In Figure 5, the complete model results are compared with the model where chemical diffusive cues are inactive. Colors represents concentrations. In both models, along the borders short--range repulsive cues are used
to keep axons confined in the computational domain. In the complete model, purple indicates an attractive zone, whilst light blue a repulsive one, with intermediate modulations. In the partial

model, purple indicates absence of chemical substances.

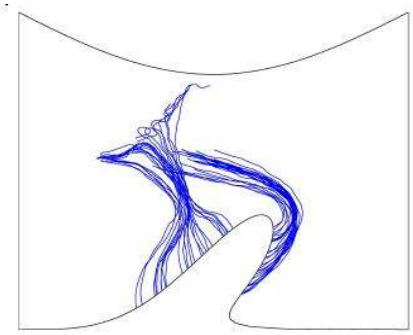

Figure 4. Axon morphology when homophilic attraction is turned off.

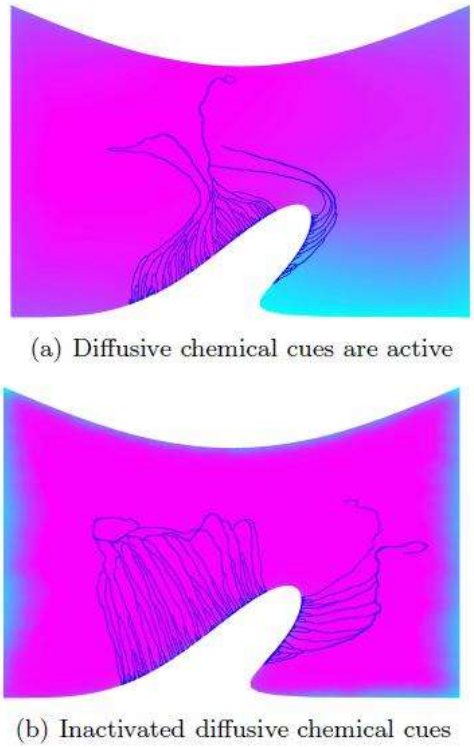

Figure 5. Axon morphology with the complete model and when chemical cues are turned off.

5. Conclusions

In this work, we have proposed a mathematical and numerical framework aimed at producing numerical simulations of axon pathfinding. We have briefly described a macroscopic model for the axon growth cone motion based on a lumped description of the filopodia dynamics.
As a further significant aspect, we have considered the deformation of the surrounding matrix. The results show the impact on the final morphology. From this point of view, a more realistic characterization of the mechanical behavior of the axons could be introduced by modeling a certain bending stiffness of the axon.
Moreover, the St. Venant--Kirchhoff model is a classical nonlinear model for compressible elastic materials. The complete model we have proposed is the superposition of the matrix movement and of the trajectory deviation due to the growth cone sensing role. In this contribution we have dealt with the 2D case; the 3D extension as well as a deeper comparative discussion with biological data will be the object of a future work.

6. References

1. B Mueller, Growth cone guidance: first steps towards a deeper understanding, Annu. Rev. Neurosci. **22**, 351-601 (1999)
2. H Song, and M M Poo, The cell biology of neuronal navigation, Nat. Cell Biol., **3**, E81–E88 (2001)
3. M Tessier-Lavigne, and C Goodman, The molecular biology of axon guidance, Science **274**, 1123-1133 (1996)
4. V Rehder, and S Kater, Filopodia on neuronal growth cones: multi-functional structures with sensory and motor capabilities. Seminars in the Neurosciences , **8**, 81-88 (1996)
5. G Aletti, P Causin, G Naldi, and M Semplice, A Multiscale Computational Model of Chemotactic Axon Guidance. In L Liu, D Wei, Y Li, and H Lei (Eds.), Handbook of Research on Computational and Systems Biology: Interdisciplinary Applications (pp. 628-645). Hershey, PA: Medical Information Science Reference (2011)
6. G Aletti, and P Causin, Mathematical characterisation of the transduction chain in growth cone pathfinding, Systems Biology IET, **2**, 150-161 (2008)
7. G Aletti, P Causin, and G Naldi, A model for axon guidance: sensing, transduction and movement, In: Collective Dynamics: Topics on Competition and Cooperation in the Biosciences (AIP Conference Proceedings Volume 1028), American Institute of Physics, Melville. NY, USA (2008)
8. S De Marchis, A Fasolo, M T Shipley, and A C Puche, Unique neuronal tracers show migration and differentiation of SVZ progenitors in organotypic slices. J. Neurobiol. **49**, 326-338 (2001)

9. S R Heidemann, P Lamoreux, R E Buxbaum, Growth cone behavior and production of traction force, J. Cell Biol., **111**, 1949-1957 (1990)

7. Acknowledgements

We wish to thank dr.F.Cavalli, dr.A.Gamba, and dr.M.Semplice for useful discussions on mathematical modeling.
We wish to thank dr.M.Gozzo, dr.G.Merlo, prof.A.Puche and dr.A.Zaghetto for helping us in gaining biological insights into axon guidance.
This work was partially supported by the MIUR PRIN2009 grant "Advanced numerical methods for evolution equations and multiscale problems"